Structural Engineering and Mechanics, *Vol. 67, No. 6 (2018) 587-601*
DOI: https://doi.org/10.12989/sem.2018.67.6.587

Damage states of yielding and collapse for elevated water tanks supported on RC frame staging

Suraj O. Lakhade*, Ratnesh Kumar[a] and Omprakash R. Jaiswal[b]

Department of Applied Mechanics, Visvesvaraya National Institute of Technology, Nagpur-440 010, India

(Received March 21, 2018, Revised June 26, 2018, Accepted June 27, 2018)

Abstract. Elevated water tanks are inverted pendulum type structures where drift limit is an important criterion for seismic design and performance evaluation. Explicit drift criteria for elevated water tanks are not available in the literature. In this study, probabilistic approach is used to determine maximum drift limit for damage state of yielding and damage state of collapse for the elevated water tanks supported on RC frame staging. The two damage states are defined using results of incremental dynamic analysis wherein a total of 2160 nonlinear time history analyses are performed using twelve artificial spectrum compatible ground motions. Analytical fragility curves are developed using two-parameter lognormal distribution. The maximum allowable drifts corresponding to yield and collapse level requirements are estimated for different tank capacities. Finally, a single fragility curve is developed which provides maximum drift values for the different probability of damage. Further, for rational consideration of the uncertainties in design, three confidence levels are selected and corresponding drift limits for damage states of yielding and collapse are proposed. These values of maximum drift can be used in performance-based seismic design for a particular damage state depending on the level of confidence.

Keywords: incremental dynamic analysis; fragility analysis; elevated water tanks; drift limits; frame staging

1. Introduction

Elevated water tanks are commonly used in public water distribution system. These tanks are generally supported on frame staging or shaft staging (Fig. 1). The elevated water tanks are considered as important structures as its uninterrupted functionality is required for water supply and firefighting during the post-earthquake scenario. However, in many of the past earthquakes, a number of such tanks were severely damaged (Steinbrugge and Flores 1963, Mehrain 1990, Astaneh and Ashtiany 1990, Jain *et al.* 1994, Saffarini 2000, Rai 2002, Rai 2003).

Reinforced concrete (RC) and steel water tanks were severely damaged in Chilean earthquake of 1960, after which researchers started working on improving the seismic design methodology of water tanks. The primary focus of the researches then was on modeling of tank container with impulsive and convective liquid mass. Various idealized models based on independent or combined consideration of water mass, container mass and flexibility of tank wall were proposed viz. one mass system, two mass system and three mass system. Applicability of these idealized models has been reported by many researchers (Sonobe and Nishikawa 1969, Shepherd 1972). Further, the effects of soil-structure interaction, fluid structure interaction and flexibility of supporting frame were also studied and various modelling techniques were proposed. With improvements in seismic design procedure and incorporation of response reduction/modification factors in seismic design codes, nonlinear deformations and damages are allowed in structures during moderate to severe seismic intensities. In case of elevated water tank, primarily the supporting structure i.e., frames or shaft staging are expected to undergo nonlinear deformations. Accordingly, the primary focus of research on elevated water tank has shifted to supporting structures (Seleemah and El-sharkawy 2011, Masoudi *et al.* 2012, Ghateh *et al.* 2015, Ghateh *et al.* 2016, Hashemi and Bargi 2016, Lakhade *et al.* 2017). Overall, the mass of supporting structure is significantly small as compared to the container and water mass; however, stiffness, strength and nonlinear behaviour of supporting structure are the primary parameters which dictate the seismic behaviour of elevated water tank. Consequently, the elevated water tanks are considered as inverted pendulum type structures. In these types of structures limiting drift is an essential criterion for design and performance evaluation. In literature it is observed that the drift limit criteria for building design and performance evaluation are well established (ASCE 7 2010, ASCE 41-13 2014, EN 1998-1:2004, IS 1893 Part 1 2002), however, for elevated water tanks, the explicit drift criteria are not available. Therefore, in this paper, the drift limits corresponding to yield and collapse of elevated water tanks are proposed. Estimation of drift limits using deterministic framework is a cumbersome and time-consuming task, thus, a simplified probabilistic procedure based on analytical fragility curve is used. Identification of threshold damage states is the key step for the development of analytical fragility curves. For buildings, researchers have predicted the threshold damage

*Corresponding author, Ph.D. Student
E-mail: surajlakhade@gmail.com
[a]Associate Professor
[b]Professor

http://www.techno-press.com/journals/sem&subpage=7
ISSN: 1225-4568 (Print), 1598-6217 (Online)

(a) (b)

Fig. 1 Elevated water tank supported on (a) reinforced concrete frame staging, (b) reinforced concrete shaft staging

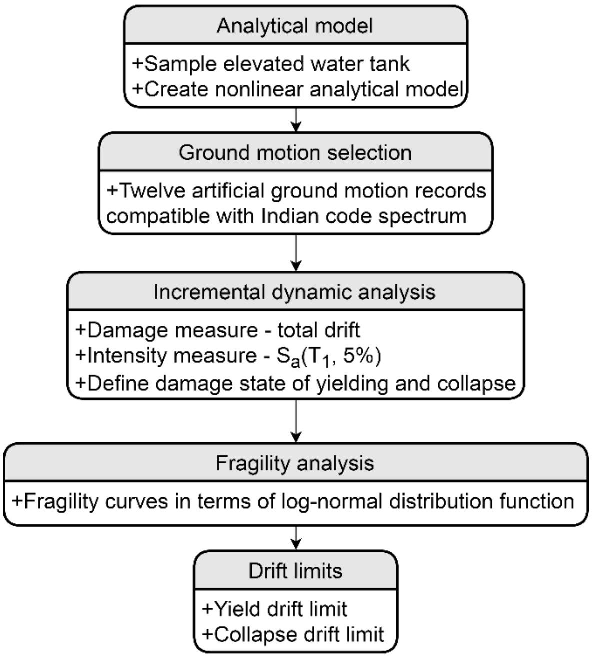

Fig. 2 Framework of present study

states to be used for analytical or hybrid fragility curves (HAZUS-MH 2011, Barbat *et al.* 2006, Giovinazzi 2005), however, no such prediction is available for elevated water tank on frame staging.

Therefore, in present study, a method based on Incremental Dynamic Analysis (IDA) (proposed by Kircil and Polat 2006) is used to estimate the threshold values corresponding to the damage state of yielding and collapse. Fig. 2 shows the framework of present study. It shall be noted that the scope of present study is limited to predicting the drift limits of only reinforced concrete elevated water tanks supported on frame staging. The selected tank models are in line with the practically constructed elevated water tanks and not exhaustive. Moreover, the effect of sloshing, empty tank condition, soil-structure interaction, vertical ground motion and amplification of ground motion due to soil has also not been considered. The study can be further extended by considering the aforementioned parameters.

2. Description of elevated water tanks

Twelve models of elevated water tank are developed in the study for four tank capacities viz. 0.09 Megaliters (Ml), 0.6 Ml, 1.7 Ml and 2.6 Ml representing the entire range of tanks (small, medium, large and very large) and three staging heights viz. 16 m, 20 m, and 24 m. Details of RC frame staging for different tank capacities are shown in Fig. 3. Four frame staging plan configurations have been selected corresponding to the four tank capacities by keeping the distance between adjacent columns constant at 3.6 m. In elevation, the intermediate braces are spaced at an interval of 4 m. The tank having a capacity of 0.09 Ml is supported on 4 columns plan configuration, similarly, the 0.6 Ml on 12 columns, 1.7 Ml on 24 columns and 2.6 Ml on 37 columns (Fig. 3).

The tanks are designed as per the requirement of IS 1893 Part 2 (2014) for the highest seismic zone, having zone factor equal to 0.36. Elevated water tank being an important structure the importance factor (I) is considered as 1.5. The soil is assumed to be hard with standard penetration test value greater than 30. Special ductility provisions as per IS 13920 (2016) are followed and response reduction factor (R) value is assumed as 4. Table 1 shows the specification of tank models and Table 2 shows the dimensions and typical reinforcement percentage for the members of the considered elevated water tanks.

2.1 Modeling of elevated water tanks

Elevated water tank mainly consists of three parts viz., tank container, supporting structure (staging) and foundation. The tank container and water inside the container can be modelled using different (Simplified) techniques which are; single degree of freedom (SDOF) system in which total mass of water, mass of container, and one third mass of staging is lumped at center of gravity of the container (Chandrasekaran and Krishna 1954, Livaoglu and Dogangun 2006, Ghateh *et al.* 2015, 2016, Hammoum *et al.* 2016, Lakhade *et al.* 2017, Maedeh *et al.* 2017c); two degree of freedom system in which a portion water is modelled as impulsive mass which is rigidly attached to the container and the other portion as convective mass (sloshing mass) which moves relative to the container wall (Housner 1963, Livaoglu and Dogangun 2006, 2007a, IITK-GSDMA 2007, Dutta *et al.* 2009, Masoudi *et al.* 2012, Hammoum *et al.* 2016, Maedeh *et al.* 2016, Maedeh *et al.* 2017a, 2017b, 2017c, Phan *et al.* 2017, Terenzi and Rossi 2018); and three degree of freedom system in which container wall flexibility effect is also considered along with impulsive and convective masses (Haroun and Housner 1981, Moslemi *et al.* 2011, Moslemi *et al.* 2016, Maedeh *et al.* 2017d, Spritzer and Guzey 2017). Additionally, the effect of soil structure interaction (SSI) also influences the modelling of elevated water tank (Veletsos and Tang 1990, Dutta *et al.*

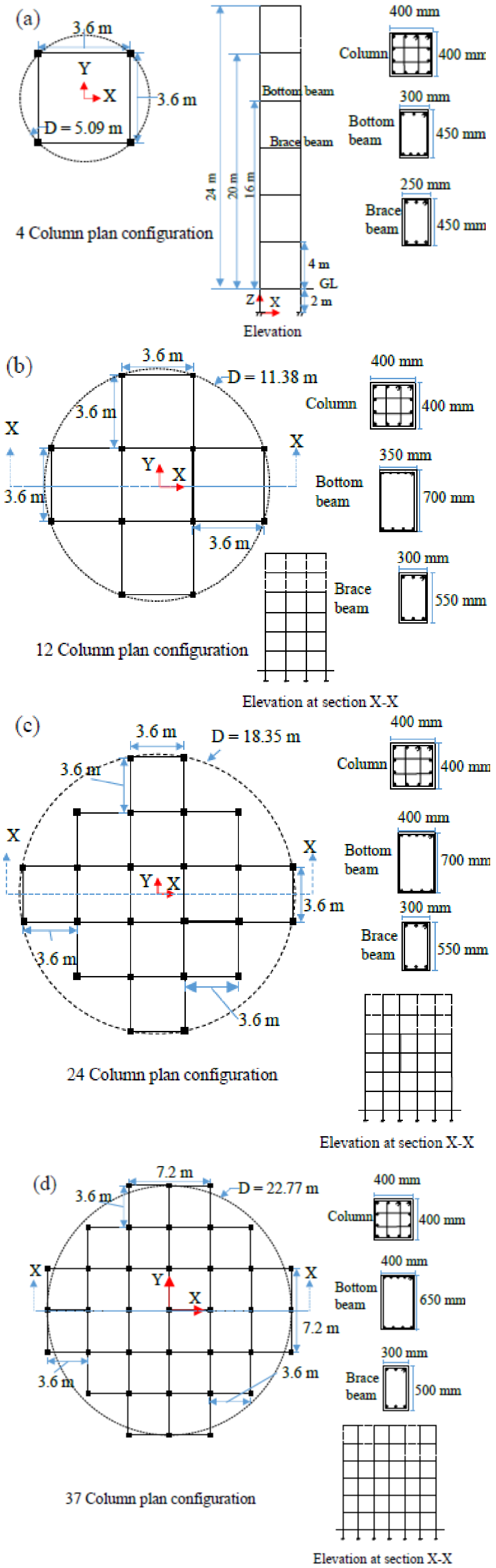

Fig. 3 Description of elevated water tanks (a) small capacity, (b) medium capacity, (c) large capacity, (d) very large capacity

Table 1 Specification of tank models

Model ID	Staging height (m)	Tank category	Tank Capacity (Ml)	Normalized base shear* (%)
16-H-0.09	16	Small	0.09	7.19
16-H-0.6		Medium	0.6	6.76
16-H-1.7		Large	1.7	6.34
16-H-2.6		Very large	2.6	6.27
20-H-0.09	20	Small	0.09	6.15
20-H-0.6		Medium	0.6	5.90
20-H-1.7		Large	1.7	5.56
20-H-2.6		Very large	2.6	5.53
24-H-0.09	24	Small	0.09	5.42
24-H-0.6		Medium	0.6	5.24
24-H-1.7		Large	1.7	4.99
24-H-2.6		Very large	2.6	4.98

*Design base shear normalized to the seismic weight

2004, Livaoglu and Dogangun 2005, 2006, 2007a, 2007b, Dutta *et al.* 2009, Livaoglu 2013, Shakib *et al.* 2010, Omidinasab and Shakib 2012, Maedeh *et al.* 2016, Maedeh *et al.* 2017a, 2017b, 2017c, Park *et al.* 2017).

In a recent study Maedeh *et al.* (2017c) compared various responses viz. natural period, base shear and overturning moment of elevated water tank modelled using six different modelling methods (i.e., single degree of freedom, coupled and uncoupled multi degree of freedom for fluid-structure interaction, as well as the mass-spring substructure method for soil-structure interaction). They concluded that fluid-structure-soil interaction (FSSI) has significant effect on response and models considering multi degree of freedom system with FSSI effect predicts precise result. However, they also concluded that maximum value of base shear occurred for SDOF and SDOF-SSI and highest overturning moment would occur for SDOF-SSI with embedment ratio 1.

Present study focuses on the drift limits, which depend on strength and stiffness of frame staging, and hence some simplifications are made while modeling the other two parts i.e., tank container with water and foundation. As indicated by Maedeh *et al.* (2017c) that the maximum value of base shear will be obtained for SDOF model (i.e., complete liquid is modelled as impulsive mass) and hence, in present study the elevated tank is modelled as SDOF system. The foundation is assumed to be resting on hard soil therefore, modelled as fixed support. It is to note that different modelling techniques may affect the drift limits proposed in this study. Further, the study can be extended to different modelling techniques to achieve better approximations.

Three-dimensional mathematical models of RC frame-stagings are developed in SAP 2000, nonlinear (2004) software. The columns and braces are modeled using frame elements. The frame element is having 6-degrees of freedom at each connecting joint with the capability of including the effect of biaxial bending, torsion, axial deformation and biaxial shear deformation. To consider the effect of tank bottom slab rigidity, the rigid diaphragm

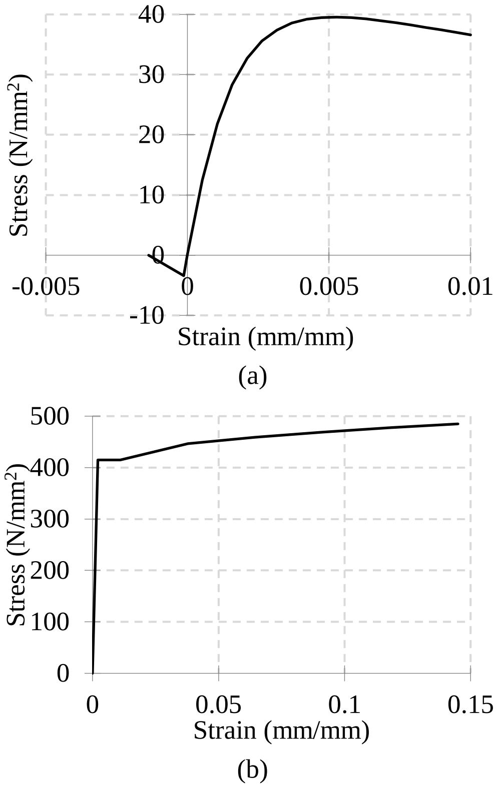

Fig. 4 Stress-strain model (a) confined concrete, (b) steel reinforcement

Table 2 Dimensions and typical reinforcement percentage for the members of tank models

Model ID	Dimensions (cm)			Reinforcement (%)		
	Bottom beam	Brace beam	Column	Bottom Beam (Top /Bot.)	Brace Beam (Top /Bot.)	Column*
16-H-0.09	30×45	25×45	40×40	0.74/0.52	0.69/0.7	2.98
16-H-0.6	35×70	30×55	40×40	0.5/0.32	0.98/0.49	2.5
16-H-1.7	40×70	30×55	40×40	0.5/0.32	0.99/0.49	2.64
16-H-2.6	40×65	30×50	40×40	0.58/0.32	1.08/0.54	2.67
20-H-0.09	30×45	25×45	40×40	0.69/0.52	0.6/0.6	2.98
20-H-0.6	35×70	30×55	40×40	0.47/0.32	0.96/0.48	2.45
20-H-1.7	40×70	30×55	40×40	0.48/0.32	0.95/0.48	2.58
20-H-2.6	40×65	30×50	40×40	0.55/0.32	1.03/0.52	2.62
24-H-0.09	30×45	25×45	40×40	0.66/0.46	0.56/0.53	2.91
24-H-0.6	35×70	30×55	40×40	0.44/0.32	0.95/0.47	2.44
24-H-1.7	40×70	30×55	40×40	0.45/0.32	0.94/0.47	2.53
24-H-2.6	40×65	30×50	40×40	0.54/0.32	1.01/0.51	2.59

*Reinforcement shown are for the columns just below the bottom beam, for lower columns the reinforcement reduces and most of the bottom columns are having only 0.8% reinforcement (minimum specified in IS 456 2000).

constraint is used.

While performing nonlinear analysis, the nonlinearity in frame elements is provided using lumped plasticity models as per FEMA 356 (2000)/ASCE 41-13 (2014). In case of braces, uncoupled moment hinges (M3) and for column members, coupled axial force and biaxial bending moment hinges (P-M2-M3), have been assigned at both the ends of the members. The concrete unconfined compressive and tensile strength are taken as 30 N/mm^2 and 3.41 N/mm^2, respectively. The stress-strain behavior for concrete as shown in Fig. 4a is defined according to Mandar's confined concrete model (Mander *et al.* 1988), and the strain limit for concrete is considered as 0.005 as per ASCE 41-13 (2014). The yield strength and ultimate strength for steel reinforcement are assumed as 415 N/mm^2 and 480 N/mm^2, respectively. The stress-strain curve of steel reinforcement is shown in Fig. 4(b) and the maximum strain were limited to 0.02 and 0.05 for longitudinal compression and tension, respectively (ASCE 41-13 2014).

In the nonlinear dynamic analysis, the choice of a suitable hysteresis model or cyclic deterioration effect is a major concern. There are different ways to include the cyclic deterioration effect in an analytical model. The one way is to consider modeling parameters based on monotonic backbone curve and clearly simulating cyclic deterioration effect. However, there is no need to define cyclic deterioration in the analytical model; if the backbone curve is provided in form of cyclic envelope curve; or if the monotonic backbone curve is modified by a predefined factor; or if the maximum deformation is constrained to the deformation corresponding to 80% of the post-peak strength (ATC 72-1 2010). ASCE 41-13 (2014) provides modified monotonic backbone curve which accounts for cyclic deterioration effect (ATC 72-1 2010). In the current study, isotropic hysteresis model along with the modified monotonic backbone curve has been adopted. In isotropic hysteresis model, plastic deformation in both the direction pushes the curve in such a way that the strength increases simultaneously in both directions. The effect of damping has been considered by mass and stiffness proportional Rayleigh damping of 5%.

3. Ground motions

Earthquake ground motions are random in nature. While performing analysis it is common to select real or artificial ground motions (EN 1998-1:2004 2004). The recommendation for selection of a number of ground motions for seismic analysis varies in literature. Since the time history analysis is computationally time-consuming, the selection of an optimum number of ground motions is important. Bazzuro and Cornell (1994) stated that for an uncoupled analysis five to seven ground motions are sufficient to quantify the hazard. For studying the seismic reliability of RC frames with uncertain drift and member capacity, Dymiotis *et al.* (1999) used only three properly selected and scaled ground motions. For probabilistic seismic demand analysis of nonlinear structures, Shome (1999) indicated that ten to twenty ground motions are generally sufficient. Erberik and Elnashai (2004) selected ten earthquake ground motion records matching with the code response spectra for studying the behavior of flat slab structures. For fragility analysis of mid-rise RC frame

Table 3 Characteristics of artificially generated ground motion records

Ground motion number	Fault Distance (km)	Peak ground acceleration (g)
GM-1	25	0.225
GM-2	25	0.186
GM-3	25	0.172
GM-4	35	0.203
GM-5	35	0.184
GM-6	35	0.188
GM-7	45	0.199
GM-8	45	0.184
GM-9	45	0.165
GM-10	55	0.211
GM-11	55	0.175
GM-12	55	0.158

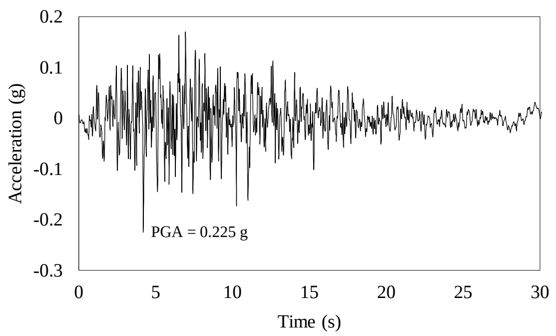

(a) GM-1

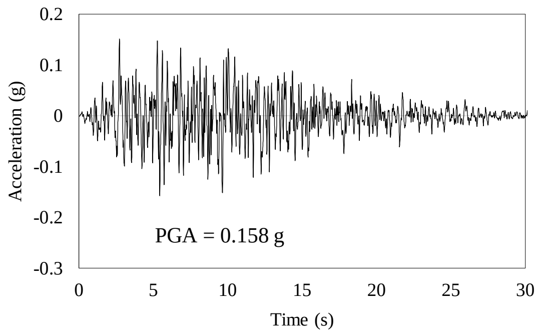

(b) GM-12

Fig. 5 Sample artificial ground motion records (a) Ground motion GM-1 (b) Ground motion GM-12

buildings, Kircil and Polat (2006) generated twelve artificial ground motions for a specific magnitude, fault distance, and duration, compatible to the site-specific demand spectra. In present study, twelve-earthquake ground motions compatible with the code response spectrum (as shown in Fig. 6) have been generated using SeismoArtif (2016).

The artificial ground motions are generated to match the elastic response spectra with 5% viscous damping of IS 1893 Part 2 (2014). The magnitude of 7.5 and duration of 30 s have been assumed for all the generated ground motions. To obtain the ground motions of different characteristics four fault distances of 25, 35, 45 and 55 km

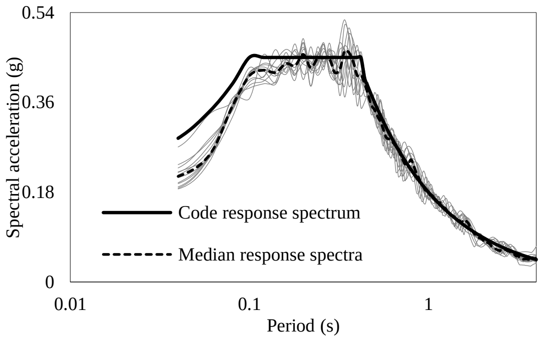

Fig. 6 Response spectra of artificially generated ground motion records

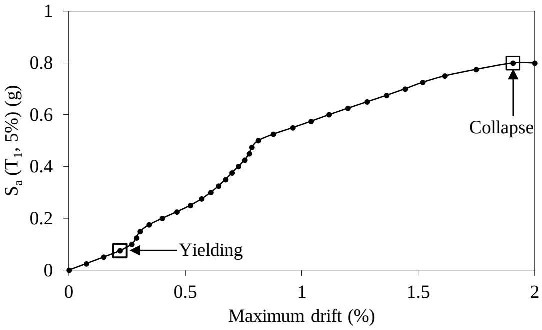

Fig. 7 Typical IDA curve for an elevated water tank of 1.7 Ml capacity subjected to artificial ground motion GM-1 to show yielding and collapse point

were considered and three ground motions corresponding to each fault distance are generated leading to a total of twelve-time histories. The soil was assumed as a generic rock with average shear wave velocity as 620 m/s. Table 3 provides the characteristics of the generated ground motion records. Artificial ground motion GM-1 and GM-12 are shown in Figs. 5(a) and (b). However, Fig. 6 shows the comparison of the elastic spectra of the artificially generated ground motion records and the code spectrum (IS 1893 Part 2 2014).

4. Incremental dynamic analysis

Incremental dynamic analysis (IDA) provides a better understanding of structural behavior under seismic loading and is generally adopted to quantify the seismic risk of structures. This technique is thoroughly discussed by Vamvatsikos and Cornell (2002a). IDA requires, carrying out a number of nonlinear dynamic analysis for a suite of scaled ground motions. The ground motions are scaled in such a way that the structure is forced from elastic to the inelastic range and ultimately to the failure (instability) of the entire structure. The output of IDA is generally a curve of damage measure (DM) versus intensity measure (IM). For present study maximum drift (%) is selected as the damage measure and the 5% damped elastic spectral acceleration at fundamental period of structure i.e., S_a (T_1, 5%) is selected as the intensity measure. The maximum drift is defined as the ratio of maximum top lateral displacement to the total height of the structure. In order to develop IDA curves, each ground motion is scaled by scaling the spectral acceleration at the fundamental period (T_1) of the structure S_a (T_1, 5%). The S_a (T_1, 5%) is scaled for the increment interval of 0.05 g, thereby, developing a suite of scaled time histories for a particular ground motion.

4.1 Damage state thresholds

Identification of appropriate damage states is the key step for development of analytical fragility curves. In the literature it has been observed that researchers have identified the damage states based either on few experiments or by judgement of experts or by closely observing the performance of structures in past earthquakes. A number of damage state threshold definitions have been presented for buildings (Giovinazzi 2005, Barbat *et al.* 2006, Kappos *et al.* 2006, HAZUS-MH 2011), however, similar damage state threshold definitions for frame staging of water tank have not been found in the literature. In absence of well-defined damage state thresholds, the IDA curves can be suitably used to define at least the yield and the collapse threshold limits. Kircil and Polat (2006) identified that from IDA curves the yield point of structure can be defined when the curve deviates from its initial linear path and the collapse point can be defined when a small increase in intensity measure will lead to an unrealistic increase in the damage measure. In present study, the method proposed by Kircil and Polat (2006) has been used to establish the damage levels corresponding damage state of yield and collapse. To take care of the variability in the two aforementioned damage state thresholds, twelve IDA curves have been generated. Further, the mean and standard deviation have been computed for yield and collapse damage state thresholds.

4.2 Observations from IDA

For each tank model, twelve IDA curves were developed which corresponds to the twelve artificially generated ground motions. A total of 2160 nonlinear time history analyses are performed to obtain 144 IDA curves. Figs. 8-10 shows IDA curves for tanks with staging height 16 m, 20 m and 24 m, respectively. The yield and collapse points for each IDA curve are marked along with the range of yielding and collapse capacities with respect to maximum drift.

The spectral acceleration at the level of yielding, S_a (T_1, 5%)$_{yield}$ and at the level of collapse, S_a (T_1, 5%)$_{collapse}$ for different tank capacities are given in Table 4 and 5. These values are obtained for the considered twelve artificial ground motions. Also, the mean and standard deviation values of S_a (T_1, 5%)$_{yield}$ and S_a (T_1, 5%)$_{collapse}$ are obtained. It is interesting to note that even though there is substantial variation in the tank capacities and the frame staging the variation among yield capacity and collapse capacity of different tanks obtained from IDA is minor. For all the considered tank models the mean value of S_a (T_1, 5%)$_{yield}$ is 0.082 g and the mean value of S_a (T_1, 5%)$_{collapse}$ is 0.67 g. Similarly, the standard deviation value for S_a (T_1, 5%)$_{yield}$ is 0.023 and for S_a (T_1, 5%)$_{collapse}$ is 0.15. For 0.09 Ml tank capacity the range of maximum drift for yield capacity is 0.06% - 0.48% and for collapse capacity is 1.45% - 1.93%. For 0.6 Ml tank capacity the range of maximum drift for yield capacity is 0.10% - 0.41% and for collapse capacity is 1.29% - 1.99%. For 1.7 Ml tank capacity the range of maximum drift for yield capacity is 0.15% - 0.61% and for collapse capacity is 1.21% - 1.92%. For 2.6 Ml tank capacity the range of maximum drift for yield capacity is

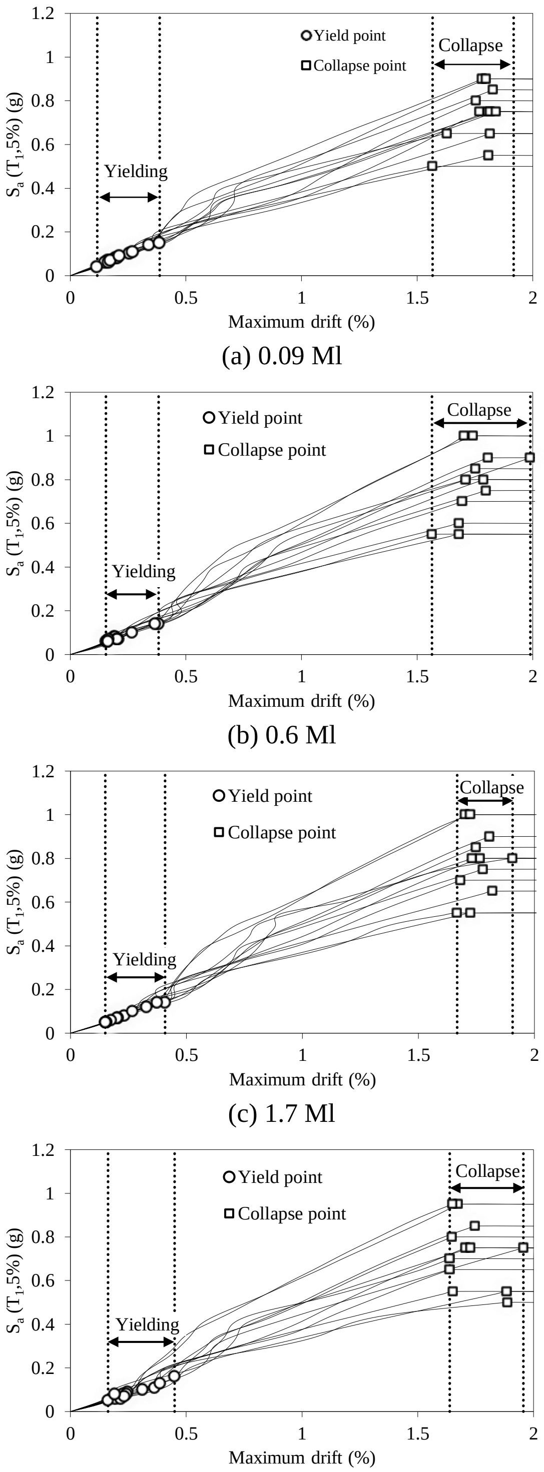

(a) 0.09 Ml

(b) 0.6 Ml

(c) 1.7 Ml

(d) 2.6 Ml

Fig. 8 IDA curves for elevated water tank with staging height 16 m

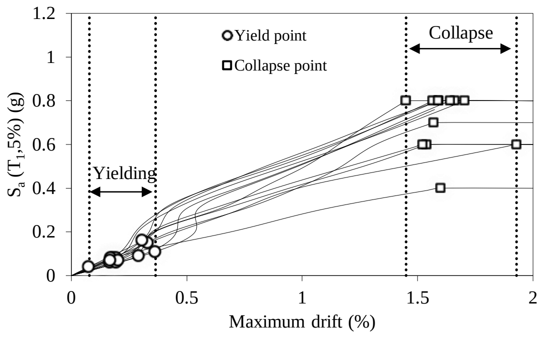

(a) 0.09 Ml

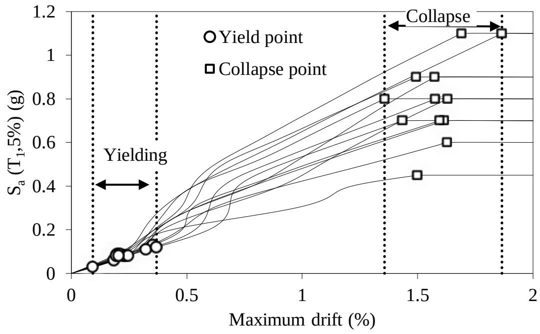

(b) 0.6 Ml

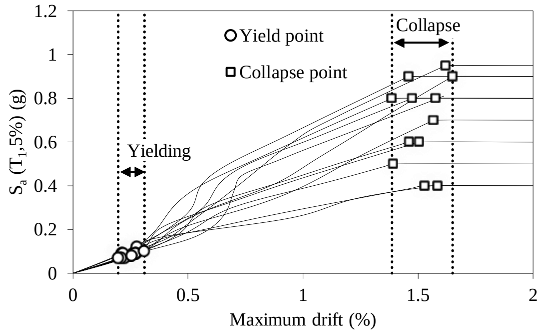

(c) 1.7 Ml

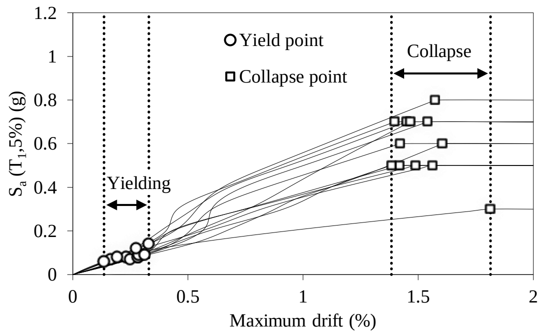

(d) 2.6 Ml

Fig. 9 IDA curves for elevated water tank with staging height 20 m

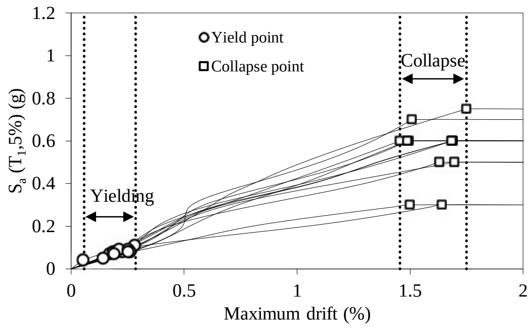

(a) 0.09 Ml

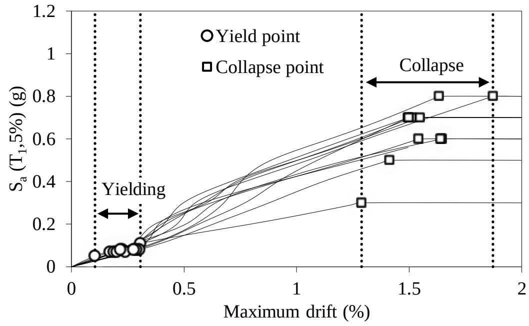

(b) 0.6 Ml

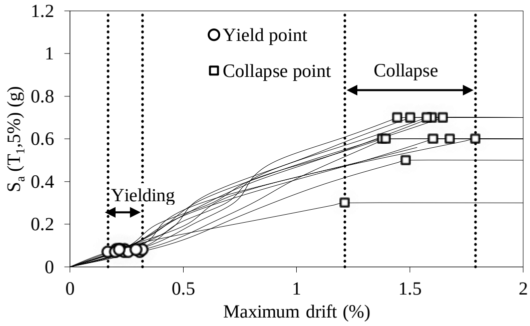

(c) 1.7 Ml

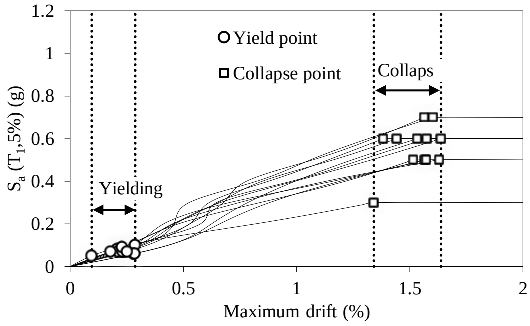

(d) 2.6 Ml

Fig. 10 IDA curves for elevated water tank with staging height 24 m

0.10% - 0.45% and for collapse capacity is 1.34% - 1.96%. The mean value of maximum drift for yield capacity and collapse capacity is 0.24% and 1.62%, respectively.

5. Fragility analysis

The seismic fragility analysis is a probabilistic method for seismic vulnerability assessment of structural components or systems (Erberik 2015). Generally, a damage probability matrix (DPM) and fragility curves are obtained from a seismic fragility analysis. DPM provides distinct values of damage state probabilities for a particular intensity measure. Whereas, fragility curves are continuous functions that represent the probability of exceeding the

Table 4 Spectral acceleration at the level of yielding for considered tank models

Ground motion number	S_a (T_1, 5%)$_{yield}$ (g)											
	Staging height = 16 m				Staging height = 20 m				Staging height = 24 m			
	Tank Capacity (Ml)				Tank Capacity (Ml)				Tank Capacity (Ml)			
	0.09	0.6	1.7	2.6	0.09	0.6	1.7	2.6	0.09	0.6	1.7	2.6
GM-1	0.07	0.08	0.08	0.09	0.14	0.07	0.08	0.07	0.08	0.07	0.08	0.07
GM-2	0.06	0.1	0.1	0.08	0.11	0.07	0.07	0.08	0.07	0.11	0.08	0.07
GM-3	0.1	0.14	0.14	0.11	0.06	0.07	0.07	0.08	0.08	0.08	0.08	0.08
GM-4	0.08	0.08	0.07	0.06	0.04	0.05	0.13	0.06	0.04	0.05	0.07	0.05
GM-5	0.14	0.14	0.14	0.08	0.08	0.08	0.09	0.14	0.08	0.07	0.08	0.16
GM-6	0.06	0.07	0.06	0.06	0.06	0.1	0.07	0.07	0.05	0.07	0.07	0.07
GM-7	0.08	0.07	0.13	0.05	0.08	0.07	0.07	0.09	0.11	0.08	0.07	0.06
GM-8	0.11	0.08	0.08	0.1	0.07	0.07	0.08	0.08	0.09	0.07	0.07	0.07
GM-9	0.19	0.07	0.07	0.13	0.07	0.12	0.07	0.08	0.09	0.076	0.07	0.07
GM-10	0.07	0.07	0.06	0.07	0.07	0.08	0.08	0.09	0.08	0.08	0.08	0.06
GM-11	0.04	0.06	0.06	0.16	0.07	0.08	0.07	0.12	0.07	0.08	0.08	0.09
GM-12	0.09	0.06	0.06	0.08	0.08	0.09	0.09	0.09	0.08	0.08	0.08	0.07
μ*	0.09	0.09	0.09	0.09	0.08	0.08	0.08	0.09	0.08	0.08	0.08	0.08
σ	0.04	0.03	0.03	0.03	0.03	0.02	0.02	0.02	0.02	0.01	0.01	0.03

* μ = mean, σ = standard deviation

Table 5 Spectral acceleration at the level of collapse for considered tank models

Ground motion number	S_a (T_1, 5%)$_{collapse}$ (g)											
	Staging height = 16 m				Staging height = 20 m				Staging height = 24 m			
	Tank Capacity (Ml)				Tank Capacity (Ml)				Tank Capacity (Ml)			
	0.09	0.6	1.7	2.6	0.09	0.6	1.7	2.6	0.09	0.6	1.7	2.6
GM-1	0.5	0.8	0.8	0.7	0.6	0.6	0.5	0.5	0.5	0.6	0.6	0.5
GM-2	0.6	1	1	0.95	0.8	0.9	0.8	0.6	0.6	0.8	0.7	0.7
GM-3	0.5	0.6	0.65	0.55	0.6	0.7	0.6	0.5	0.5	0.6	0.6	0.5
GM-4	0.3	0.6	0.55	0.5	0.4	0.45	0.4	0.3	0.3	0.3	0.3	0.3
GM-5	0.8	1	1	0.95	0.8	1.1	0.9	0.8	0.6	0.7	0.7	0.6
GM-6	0.5	0.55	0.55	0.5	0.6	0.7	0.6	0.5	0.3	0.6	0.6	0.5
GM-7	0.5	0.7	0.7	0.65	0.7	0.8	0.7	0.5	0.75	0.5	0.5	0.5
GM-8	0.7	0.85	0.9	0.85	0.8	1.1	0.8	0.7	0.6	0.7	0.6	0.6
GM-9	0.6	0.75	0.75	0.75	0.8	0.8	0.4	0.6	0.6	0.64	0.7	0.6
GM-10	0.7	0.8	0.8	0.75	0.8	0.9	0.9	0.7	0.6	0.7	0.6	0.6
GM-11	0.7	0.85	0.85	0.8	0.8	0.8	0.95	0.7	0.6	0.7	0.7	0.6
GM-12	0.7	0.9	0.8	0.75	0.8	0.7	0.8	0.7	0.7	0.8	0.7	0.7
μ*	0.59	0.78	0.78	0.73	0.71	0.80	0.70	0.59	0.55	0.64	0.61	0.56
σ	0.14	0.15	0.15	0.15	0.13	0.19	0.19	0.14	0.14	0.14	0.12	0.11

*μ = mean, σ = standard deviation

predefined limit state for specific levels of ground motion intensity.

The fragility curves can be classified into four categories as empirical fragility curves, expert fragility curves, analytical fragility curves and hybrid fragility curves (Rossetto and Elnashai 2003). Analytical fragility curves are established from the numerical models and are generally preferred in the absence of experimental or field data of the damaged structures from past earthquakes (Ji *et al.* 2007, Pejovic and Jankovic 2016). The common form of analytical seismic fragility function is lognormal distribution function as shown in Eq. (1) (Erberik and Elnashai 2004, Kircil and Polat 2006, Rajeev and Tesfamariam 2012a, 2012b, Pejovic and Jankovic 2016, Khaloo *et al.* 2016).

Table 6 Parameters of fragility curves (λ, ζ)

Tank Capacity (Ml)	Staging height (m)	Damage level			
		Yielding		Collapse	
		λ	ζ	λ	ζ
0.09 ML	16	1.43	0.41	3.59	0.18
	20	1.71	0.39	3.79	0.26
	24	1.88	0.27	3.85	0.29
0.6 Ml	16	1.42	0.29	3.67	0.20
	20	1.69	0.38	3.95	0.25
	24	1.85	0.18	3.96	0.26
1.7 Ml	16	1.51	0.34	3.73	0.20
	20	1.80	0.16	3.86	0.31
	24	1.90	0.07	3.96	0.24
2.6 Ml	16	1.62	0.34	3.75	0.22
	20	1.89	0.23	3.79	0.26
	24	1.91	0.18	3.96	0.23

$$P(\leq D) = \Phi\left(\frac{\ln X - \lambda}{\zeta}\right) \tag{1}$$

where, Φ is the standard normal distribution, X is ground motion intensity measure (i.e., S_d, S_a, PGA), λ is the mean and ζ is the standard deviation of ln X. In absence of extensive experimental data or field observation on the level of damage in elevated water tanks subjected to different ground motions, the analytical fragility curves can be a useful tool to provide its seismic performance. The parameters of fragility curve (λ and ζ), for each damage level and different tank capacities are shown in Table 6. Fragility curve at damage level of collapse for 1.7 Ml tank capacity and 16 m staging height is shown in Fig. 11. It is to note that the either of the three i.e., S_d, S_a, PGA can be used as intensity measure for plotting the graph, however, in present case it has been observed that S_d provide more comprehendible observations therefore the same has been used.

5.1 Comparison of fragility curves with respect to staging height

The fragility curves are compared for the three staging heights i.e., 16 m, 20 m and 24 m at the damage state of yielding and damage state of collapse. It can be observed from the fragility curves shown in Figs. 12 and 13 for damage state of yielding and collapse, respectively, that for all the considered tank capacities, the spectral displacement

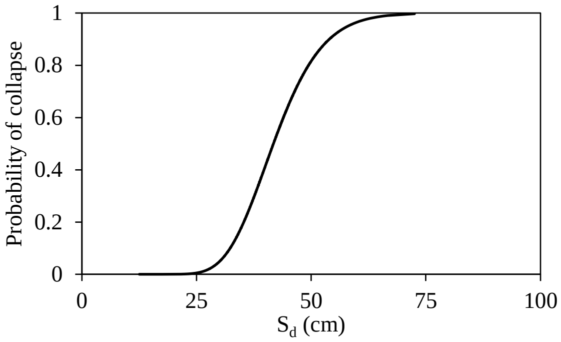

Fig. 11 Fragility curve at damage level of collapse for 1.7 Ml tank capacity and 16 m staging height

increases with increase in staging height, which is consistent to the relative change of stiffness.

5.2 Comparison of fragility curves with respect to tank capacity

The fragility curves are compared with respect to tank capacity at the considered damage state of yielding and damage state of collapse. A comparison of fragility curves for different tank capacities at damage state of yielding is shown in Fig. 14. It has been observed from the figure that at the damage level of yielding for all the considered tanks, fragility curves show marginal variation with respect to tank capacity. Also, for a particular spectral displacement value, the probability of yielding does not show any trend of variation with respect to tank capacity. It can be said from the results that the seismic behavior of the considered elevated tanks are almost same up to the damage state of yielding. Fig. 15 shows a variation of fragility curve with respect to tank capacity at damage state of collapse. It has been observed from the figure that at the damage level of collapse for all the considered tanks, fragility curves show minimal variation with respect to tank capacity.

6. Drift limits for performance-based design

Presently no guidelines are available in literature which provides drift limits of elevated water tank corresponding to various performance levels. These performance levels are used in performance-based design and for approximate evaluation of structures. Generally, the performance criteria are specified in the form of limiting values of inter-storey drift, maximum drift, spectral displacement, etc. for a particular performance level. In this study the performance criteria are determined in terms of maximum drift (%) for the established damage states of yielding and collapse of elevated water tanks.

The fragility curves with reference to maximum drift (%) are developed for the considered tank capacities at damage state of yielding and collapse as shown in Figs. 16 and 17, respectively. It should be noted that each fragility curve is developed from the mean and standard deviation of twelve values of maximum drift corresponding to a particular damage state obtained from IDA. Hence, the range of variation of maximum drift (%) for the different tank capacities can be established from the curves.

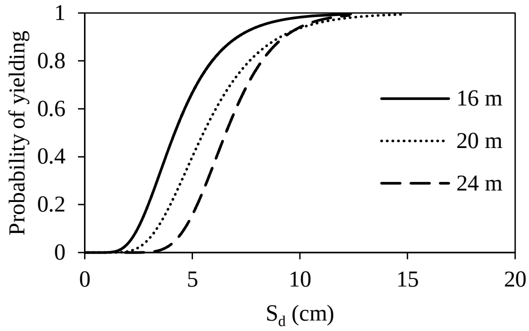

(a) 0.09 Ml

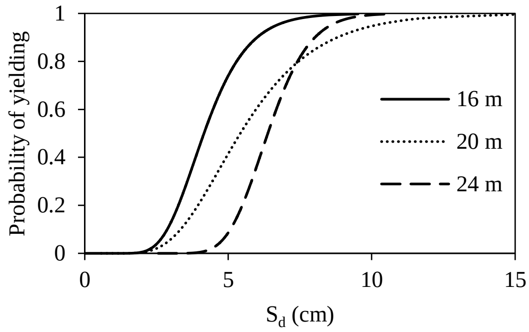

(b) 0.6 Ml

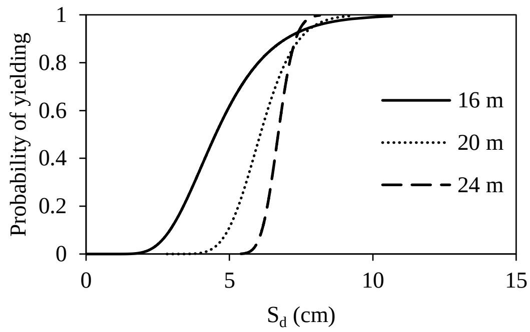

(c) 1.7 Ml

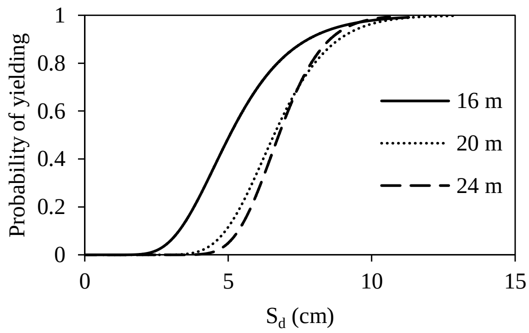

(d) 2.6 Ml

Fig. 12 Variation of fragility curve with respect to staging height at damage state of yielding

It can be observed from Fig. 16 that the probability of yielding is similar for the elevated water tanks with different staging heights. However, for probability of collapse the elevated water tanks with lower staging height show relatively good performance (Fig. 17). Table 7 shows

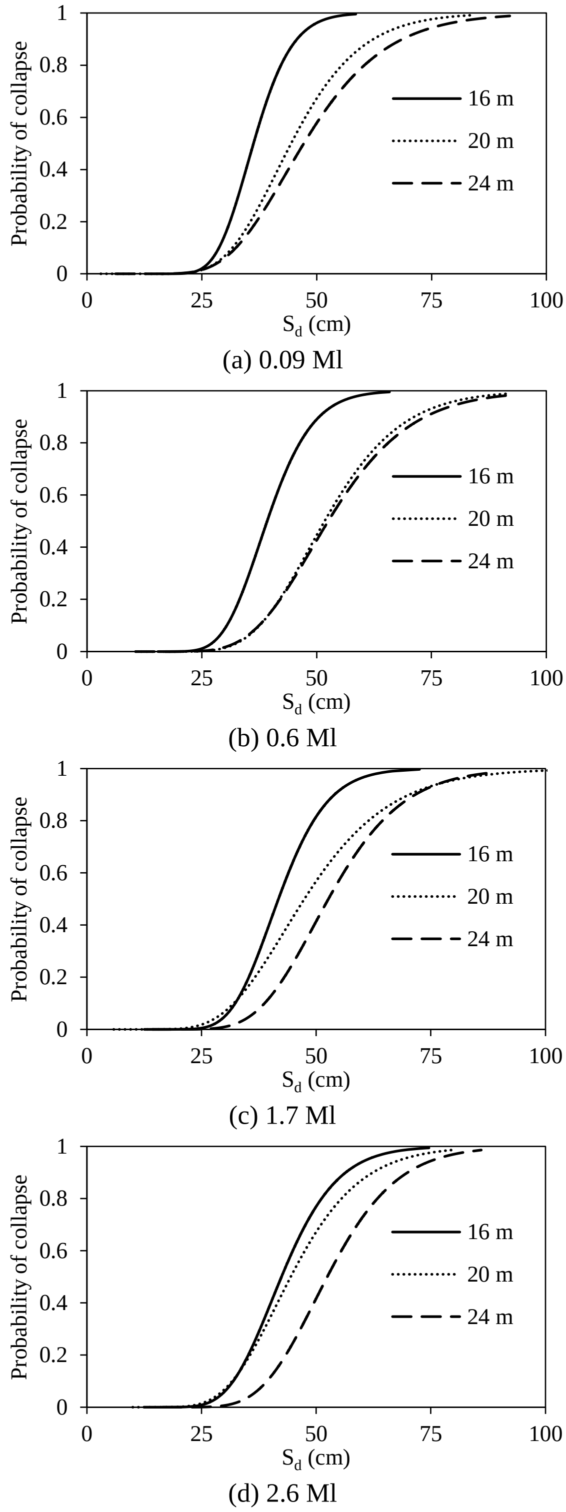

Fig. 13 Variation of fragility curve with respect to staging height at damage state of collapse

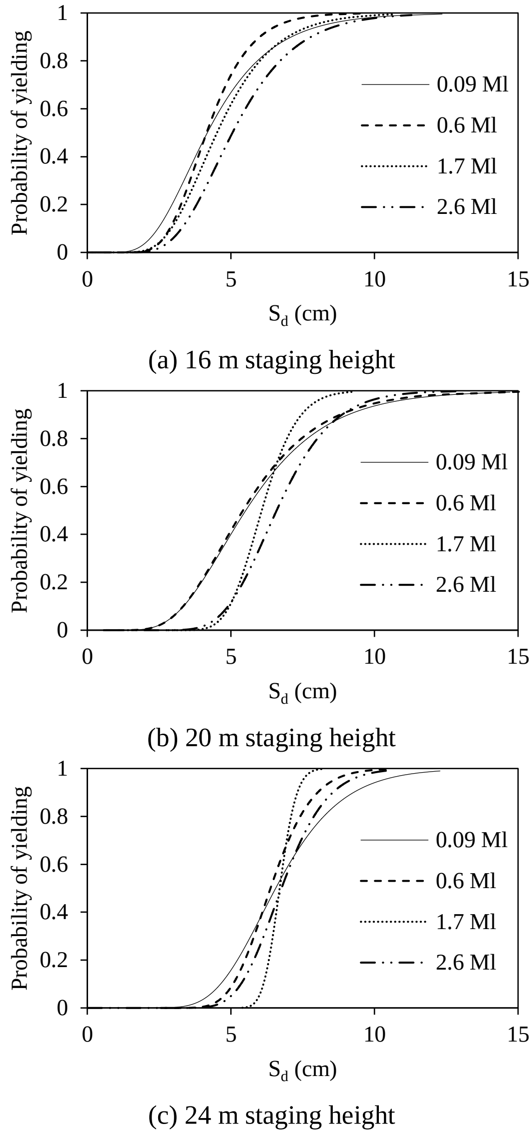

Fig. 14 Variation of fragility curve with respect to tank capacity at damage state of yielding

maximum drift (%) at different probability values i.e., 5%, 25% and 50% for damage state of yielding and collapse. For all the considered tanks, at 50% probability of both yielding and collapse the mean value of maximum drift is around 0.22% and 1.62%, respectively. However, these values reduce to approximately 0.14% and 1.45% for 5% probability of yielding and collapse, respectively.

The fragility curves vary with tank capacities but do not show any trend in variation. This may be due to the complex variation of demand parameters such as earthquake ground motion records and the structural parameters such as the dimensions, grade of concrete, grade of steel, etc. Hence, single fragility curve is developed for each damage state i.e., yielding and collapse. The parameters for fragility curve are obtained from the results of 144 maximum drift values corresponding to each damage state, obtained by IDA on the considered twelve elevated water tanks. The method proposed by Kircil and Polat (2006) is used to prepare a single fragility curve. In this method, the lognormal plot of *ln X* (maximum drift) and corresponding standard normal variable (s) are plotted and a linear regression analysis is carried out to obtain the mean and standard deviation. Figs. 18(a) and (b) shows a plot of lognormally distributed maximum drift versus standard normal variable for damage state of yielding and collapse, respectively.

The standard normal variable (s) is calculated as per Eq.

Table 7 Yield and collapse drift (%) at different probability values for damage state of yielding and collapse

Capacity	Staging height	Drift (%)					
		Probability of yielding			Probability of collapse		
		5%	25%	50%	5%	25%	50%
0.09 Ml	16 m	0.11	0.17	0.21	1.64	1.73	1.80
	20 m	0.11	0.15	0.19	1.43	1.54	1.61
	24 m	0.10	0.14	0.19	1.44	1.53	1.60
0.6 Ml	16 m	0.13	0.17	0.21	1.58	1.67	1.74
	20 m	0.14	0.18	0.21	1.38	1.49	1.58
	24 m	0.13	0.18	0.22	1.33	1.46	1.55
1.7 Ml	16 m	0.12	0.17	0.22	1.63	1.71	1.76
	20 m	0.17	0.20	0.23	1.38	1.46	1.52
	24 m	0.17	0.21	0.24	1.28	1.42	1.52
2.6 Ml	16 m	0.15	0.21	0.26	1.56	1.65	1.71
	20 m	0.16	0.20	0.25	1.33	1.43	1.51
	24 m	0.13	0.18	0.23	1.38	1.46	1.53

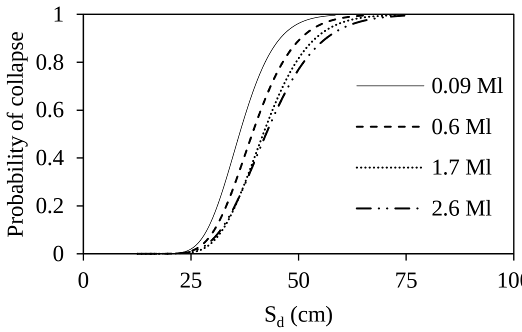

(a) 16 m staging height

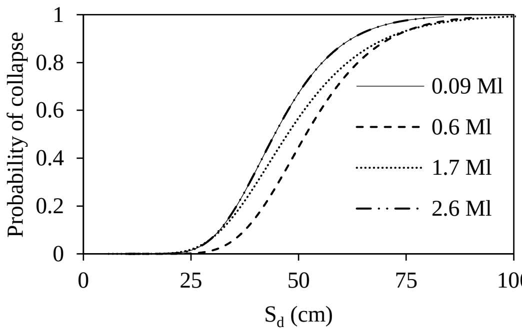

(b) 20 m staging height

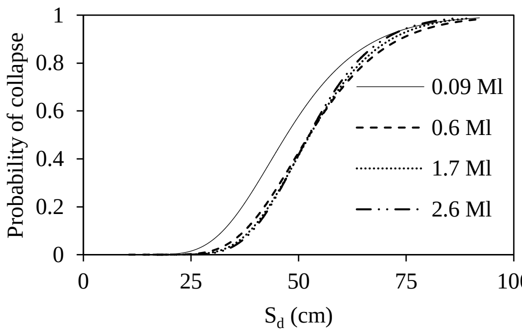

(c) 24 m staging height

Fig. 15 Variation of fragility curve with respect to tank capacity at damage state of collapse

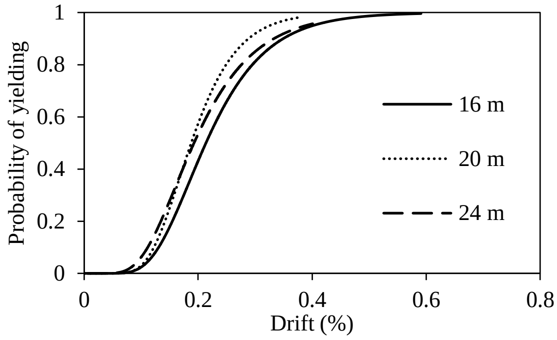

(a) 0.09 Ml

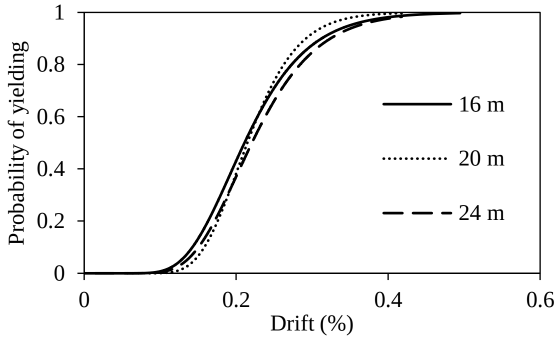

(b) 0.6 Ml

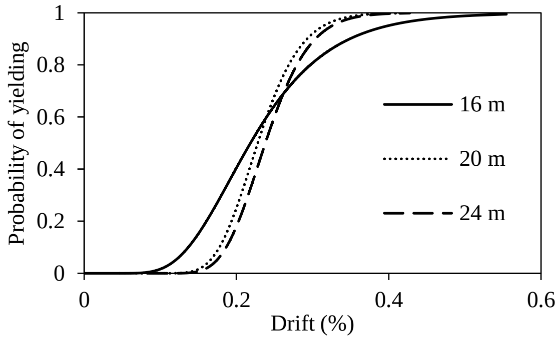

(c) 1.7 Ml

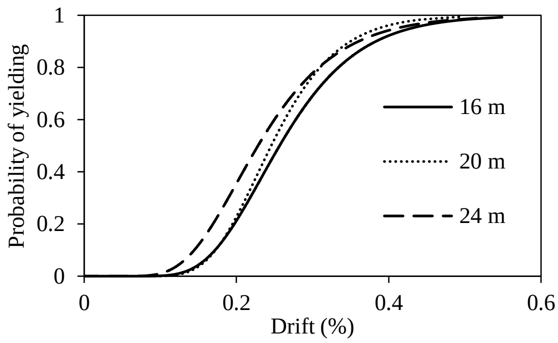

(d) 2.6 Ml

Fig. 16 Fragility curves for the probability of yielding

(2), where the terms λ and ζ are mean and standard deviation of *ln X* and are indicated on Figs. 18(a) and (b).

$$s = \frac{\ln X - \lambda}{\zeta} \tag{2}$$

Figs. 19(a) and (b) show plot of the probability of yielding and collapse developed at three confidence levels i.e., 5%, 50%, and 95%. Table 8 provides the values of

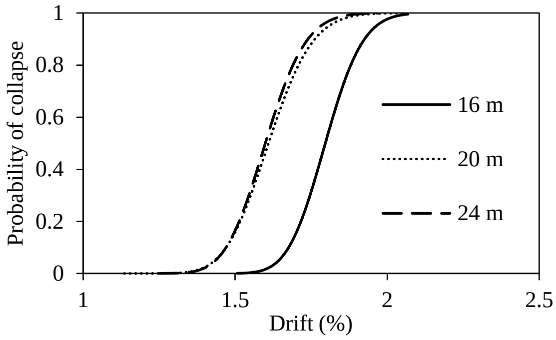

(a) 0.09 Ml

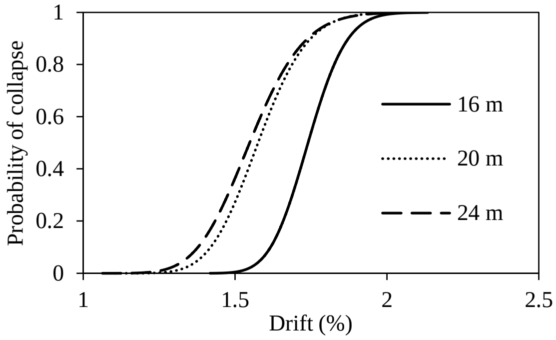

(b) 0.6 Ml

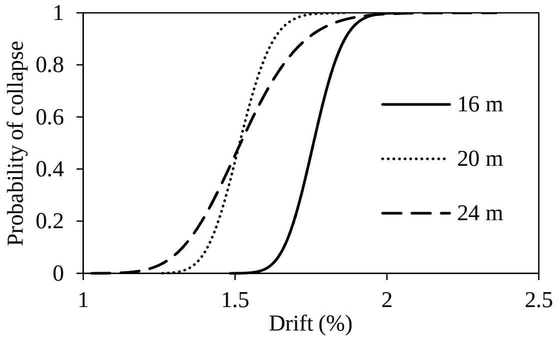

(c) 1.7 Ml

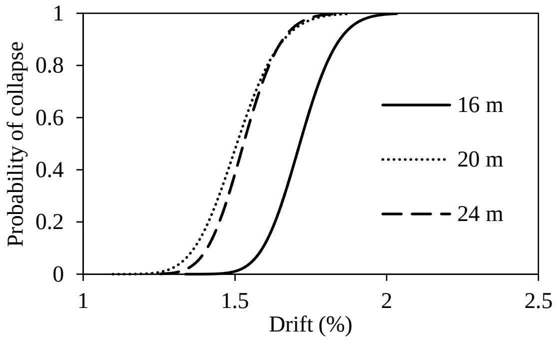

(d) 2.6 Ml

Fig. 17 Fragility curves for the probability of collapse

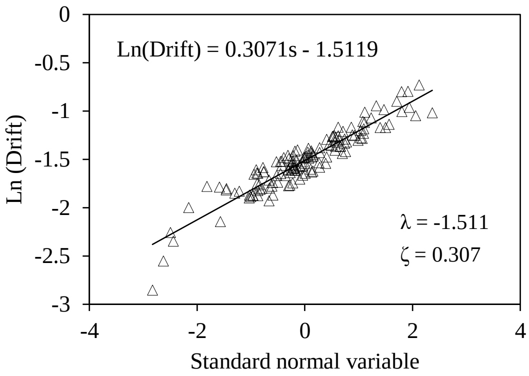

(a) Probability of yielding

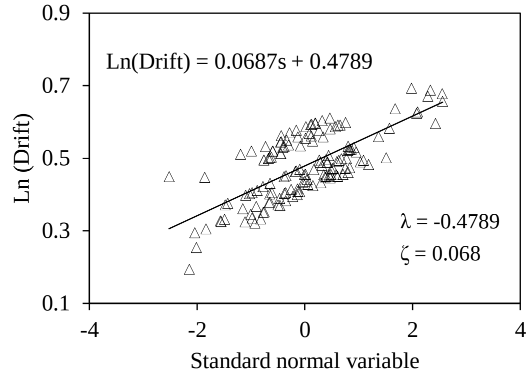

(b) Probability of collapse

Fig. 18 Plot of lognormal distributed maximum drift versus standard normal variable

Table 8 Yield and collapse drift (%) at different probability yielding and collapse at three confidence levels

Confidence level	Probability of yielding			Probability of collapse		
	5%	25%	50%	5%	25%	50%
95%	0.123	0.166	0.203	1.414	1.510	1.583
50%	0.132	0.178	0.215	1.434	1.530	1.601
5%	0.136	0.181	0.221	1.441	1.540	1.612

maximum drift for both the damage state of yielding and collapse at a different level of confidence. Hence, in case of performance-based design, for a particular damage state depending on the level of confidence, an appropriate value of maximum d rift can be chosen from the table. Moreover, these limits can also be used in the approximate evaluation of the elevated water tanks supported on frame staging.

7. Conclusions

Drift criteria for performance estimation of elevated water tanks supported on RC frame staging are not readily available in codes and literature. In present study, maximum drift limits corresponding to two damage states i.e., yielding and collapse are determined. In order to establish the damage state thresholds for yielding and collapse, 144 IDA curves based on 2160 nonlinear time history analysis are developed. Four tank capacities of 0.09 Ml, 0.6 Ml, 1.7 Ml and 2.6 Ml, and three staging height of 16 m, 20 m, and 24 m are considered covering the range of practically constructed elevated water tanks. Fragility curves are developed using damage state thresholds obtained from IDA. Maximum drift value for the damage state of yielding and collapse is determined. It has been observed from results that for the water tanks designed as per code provisions, variation in fragility curves pertaining to staging height and tank capacity at the respective damage state of yielding and collapse is small. Therefore, drift limit of

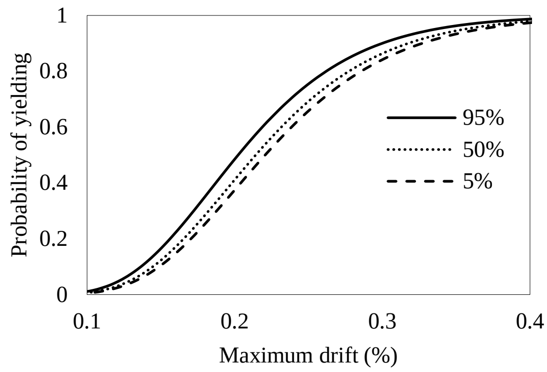

(a) Yielding

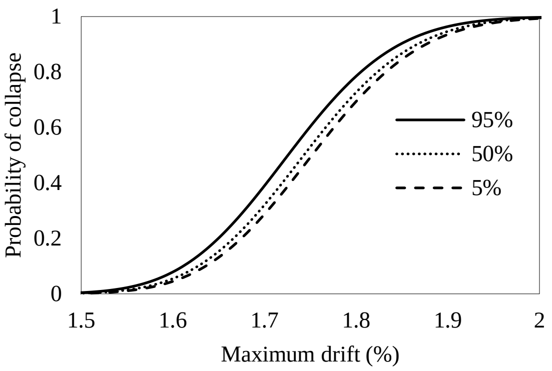

(b) Collapse

Fig. 19 Fragility curves for two damage states

appropriately designed elevated water tanks can be generalized. Based on the above conclusion, a single fragility curve combining the results of all tanks at three confidence level is developed which provides maximum drift values for the different probability of damage. Drift limit of elevated water tank on RC frame staging for damage state of yielding and collapse ranges from 0.12% to 0.22% and 1.4% to 1.61%, respectively. However, for a stringent condition i.e., the drift limits for 95% confidence and 5% probability corresponding to damage state of yielding and collapse is limited to 0.123% and 1.414%, respectively. Proposed maximum drift limits can be used in performance-based design for a particular damage state and level of confidence.

References

ASCE 41-13 (2014), *Seismic Rehabilitation of Existing Buildings*, *American Society of Civil Engineers*, Reston, Virginia, U.S.A.

ASCE 7 (2010), *Minimum Design Loads for Buildings and Other Structures*, American Society of Civil Engineers, Reston, Virginia, U.S.A.

Astaneh, A. and Ashtiany, M.G. (1990), *The Manjil, Iran, Earthquake of June 1990*, Report No. 24(12), Earthquake Engineering Research Institute, California, U.S.A.

ATC 40 (1996), *Seismic Evaluation and Retrofit of Concrete Buildings*, Applied Technology Council, Redwood City, California, U.S.A.

ATC 72-1 (2010), *Modeling and Acceptance Criteria for Seismic Design and Analysis of Tall Buildings*, Applied Technology Council, California, U.S.A.

Barbat, A.H., Pujades, L.G. and Lantada, N. (2006), "Performance of buildings under earthquakes in Barcelona, Spain", *Comput.-Aid. Civil Infrastruct. Eng.*, **21**(3), 573-593.

Bazzurro, P. and Cornell, C.A. (1994), "Seismic hazard analysis of nonlinear structures. I: Methodology", *J. Struct. Eng.*, **120**(11), 3320-3344.

Chandrasekaran, A.R. and Krishna, J. (1954), "Water towers in seismic zones," *Proceedings of the 3rd World Conference Earthquake Engineering*, Auckland and Wellington, New Zealand.

Dutta, S., Mondal, A. and Dutta, S.C. (2004), "Soil structure interaction in dynamic behaviour of elevated tanks with alternate frame staging configurations", *J. Sound Vibr.*, **277**, 825-853.

Dutta, S.C., Dutta, S. and Roy, R. (2009), "Dynamic behavior of R/C elevated tanks with soil-structure interaction", *Eng. Struct.*, **31**(11), 2617-2629.

Dymiotis, C., Kappos, A.J. and Chryssanthopoulos, M.K. (1999), "Seismic reliability of RC frames with uncertain drift and member capacity", *J. Struct. Eng.*, **125**(9), 1038-1047.

EN 1998-1:2004 (2004), *Eurocode 8: Design of Structures for Earthquake Resistance. Part 1: General Rules, Seismic Actions and Rules for Buildings*, European Committee for Standardization, Brussels, Belgium.

Erberik, M.A. (2015), "Seismic fragility analysis", *Encyclopaed. Earthq. Eng.*, 1-10.

Erberik, M.A. and Elnashai, A.S. (2004), "Fragility analysis of flat-slab structures", *Eng. Struct.*, **26**(7), 937-948.

FEMA 356 (2000), *Commentary for the Seismic Rehabilitation of Buildings*, Federal Emergency Management Agency, Washington, U.S.A.

Ghateh, R., Kianoush, M.R. and Pogorzelski, W. (2015), "Seismic response factors of reinforced concrete pedestal in elevated water tanks", *Eng. Struct.*, **87**, 32-46.

Ghateh, R., Kianoush, R. and Pogorzelski, W. (2016), "Response modification factor of elevated water tanks with reinforced concrete pedestal", *Struct. Infrastruct. Eng.*, **12**(8), 936-948.

Giovinazzi, S. (2005), "The vulnerability assessment and the damage scenario in seismic risk analysis", Ph.D. Dissertation, Technical University Carolo-Wilhelmina at Braunschweig, Germany and University of Florence, Florence, Italy.

Hammoum, H., Bouzelha, K. and Slimani, D. (2016), *Seismic Risk of RC Water Storage Elevated Tanks: Case Study*, In Handbook of Materials Failure Analysis with Case Studies from the Chemicals, Concrete and Power Industries, 1st Edition, Elsevier, Waltham, U.S.A.

Haroun, M.A. and Housner, G.W. (1981), "Seismic design of liquid storage tanks", *ASCE J. Tech. Councils*, **107**(1), 191-207.

Hashemi, M. and Bargi, K. (2016), "An investigation about effects of fluid-structure-soil interaction on response modification coefficient of elevated concrete tanks", *Eng. Struct. Technol.*, **8**(1), 1-7.

HAZUS-MH (2011), *Multi-Hazard Loss Estimation Methodology: Earthquake Model HAZUS-MH MR5 Technical Manual*, Federal Emergency Management Agency, Washington, U.S.A.

Housner, G.W. (1963), "The dynamic behavior of water tanks", *Bullet. Seismol. Soc. Am.*, **53**(2), 381-387.

IITK-GSDMA (2007), *IITK-GSDMA Guidelines for Seismic Design of Liquid Storage Tanks*, Gujarat State Disaster Management Authority, Gandhinagar, India.

IS 13920 (2016), *Ductile Detailing of Reinforced Concrete Structures Subjected to Seismic Forces-Code of Practice*, Bureau of Indian Standard, New Delhi, India.

IS 1893 Part 1 (2002), *Criteria for Earthquake Resistant Design of Structures: Part 1 General Provisions and Buildings*, Bureau of

Indian Standard, New Delhi, India.

IS 1893 Part 2 (2014), *Criteria for Earthquake Resistant Design of Structures Part 2 Liquid Retaining Tanks*, Bureau of Indian Standards, New Delhi, India.

IS 456 (2000), *Plain and Reinforced Concrete-Code of Practice*, Bureau of Indian Standards, New Delhi, India.

Jain, S.K., Murty, C.V.R., Chandak, N., Seeber, L. and Jain, N.K. (1994), *The September 29, 1993, m6.4 killari, Maharashtra Earthquake in Central India*, Report No. 28(1), Earthquake Engineering Research Institute, California, U.S.A.

Ji, J., Elnashai, A.S. and Kuchma, D.A. (2007), "An analytical framework for seismic fragility analysis of RC high-rise buildings", *Eng. Struct.*, **29**(12), 3197-3209.

Kappos, A.J., Panagopoulos, G., Panagiotopoulos, C. and Penelis, G. (2006), "A hybrid method for the vulnerability assessment of R/C and URM buildings", *Bullet. Earthq. Eng.*, **4**(4), 391-413.

Khaloo, A., Nozhati, S. and Masoomi, H. and Faghihmaleki, H. (2016), "Influence of earthquake record truncation on fragility curves of RC frames with different damage indices", *J. Build. Eng.*, **7**, 23-30.

Kircil, M.S. and Polat, Z. (2006), "Fragility analysis of mid-rise R/C frame buildings", *Eng. Struct.*, **28**(9), 1335-1345.

Lakhade, S.O., Kumar, R. and Jaiswal, O.R. (2017), "Estimation of response reduction factor of RC frame staging in elevated water tanks using nonlinear static procedure", *Struct. Eng. Mech.*, **62**(2), 209-224.

Livaoglu, R. (2013), "Soil interaction effects on sloshing response of the elevated tanks", *Geomech. Eng.*, **5**(4), 283-297.

Livaoglu, R. and Dogangun, A. (2005), "Seismic evaluation of fluid-elevated tank-foundation/soil systems in frequency domain", *Struct. Eng. Mech.*, **21**(1), 101-119.

Livaoglu, R. and Dogangun, A. (2006), "Simplified seismic analysis procedures for elevated tanks considering fluid-structure-soil interaction", *J. Flu. Struct.*, **22**(3), 421-439.

Livaoglu, R. and Dogangun, A. (2007a), "Effect of foundation embedment on seismic behavior of elevated tanks considering fluid-structure-soil interaction", *Soil Dyn. Earthq. Eng.*, **27**(9), 855-863.

Livaoglu, R. and Dogangun, A. (2007b), "Seismic behaviour of cylindrical elevated tanks with a frame supporting system on various subsoil", *Ind. J. Eng. Mater. Sci.*, **14**, 133-145.

Maedeh, P.A., Ghanbari, A. and Wu, W. (2016), "Analytical assessment of elevated tank natural period considering soil effects", *Coupled Syst. Mech.*, **5**(3), 223-234.

Maedeh, P.A., Ghanbari, A. and Wu, W. (2017a), "New coefficients to find natural period of elevated tanks considering fluid-structure-soil interaction effects", *Geomech. Eng.*, **12**(6), 949-963.

Maedeh, P.A., Ghanbari, A. and Wu, W. (2017b), "Investigation of soil structure interaction and wall flexibility effects on natural sloshing frequency of vessels", *Civil Eng. J.*, **3**(1), 45-56.

Maedeh, P.A., Ghanbari, A. and Wu, W. (2017c), "A new analytical model for natural period analysis of elevated tanks considering fluid-structure-soil interaction", *J. GeoEng.*, **12**, 1-12.

Maedeh, P.A., Ghanbari, A. and Wu, W. (2017d), "Estimation of elevated tanks natural period considering fluid-structure-soil interaction by using new approaches", *Earthq. Struct.*, **12**(2), 145-152.

Mander, J.B., Priestley, M.J. and Park, R. (1988), "Theoretical stress-strain model for confined concrete", *J. Struct. Eng.*, **114**(8), 1804-1826.

Masoudi, M., Eshghi, S. and Ghafory-Ashtiany, M. (2012), "Evaluation of response modification factor (R) of elevated concrete tanks", *Eng. Struct.*, **39**, 199-209.

Mehrain, M. (1990), *Reconnaissance Report on the Northern Iran earthquake of June 21, 1990*, Research Report No. NCEER-90-0017, National Center for Earthquake Engineering Research, State University of New York at Buffalo, New York, U.S.A.

Moslemi, M., Ghaemmaghami, A.R. and Kianoush, M.R. (2016), "Parametric based study for design of liquid-filled elevated tanks", *Can. J. Civil Eng.*, **43**(7), 619-630.

Moslemi, M., Kianoush, M.R. and Pogorzelski, W. (2011), "Seismic response of liquid-filled elevated tanks", *Eng. Struct.*, **33**(6), 2074-2084.

Omidinasab, F. and Shakib, H. (2012), "Seismic response evaluation of the RC elevated water tank with fluid-structure interaction and earthquake ensemble", *KSCE J. Civil Eng.*, **16**(3), 366-376.

Park, H.J., Ha, J.G., Kwon, S.Y., Lee, M.G. and Kim, D.S. (2017), "Investigation of the dynamic behaviour of a storage tank with different foundation types focusing on the soil-foundation-structure interactions using centrifuge model tests", *Earthq. Eng. Struct. Dyn.*, **46**(14), 2301-2316.

Pejovic, J. and Jankovic, S. (2016), "Seismic fragility assessment for reinforced concrete high-rise buildings in Southern Euro-Mediterranean zone", *Bullet. Earthq. Eng.*, **14**(1), 185-212.

Phan, H.N., Paolacci, F., Bursi, O.S. and Tondini, N. (2017), "Seismic fragility analysis of elevated steel storage tanks supported by reinforced concrete columns", *J. Loss Prevent. Proc. Industr.*, **47**, 57-65.

Rai, D.C. (2002), "Elevated tanks", *Earthq. Spectr.*, **18**(S1), 279-295.

Rai, D.C. (2003), "Performance of elevated tanks in mw 7.7 bhuj earthquake of January 26^{th}, 2001", *J. Earth Syst. Sci.*, **112**(3), 421-429.

Rajeev, P. and Tesfamariam, S. (2012a), "Seismic fragilities of non-ductile reinforced concrete frames with consideration of soil structure interaction", *Soil Dyn. Earthq. Eng.*, **40**, 78-86.

Rajeev, P. and Tesfamariam, S. (2012b), "Seismic fragilities for reinforced concrete buildings with consideration of irregularities", *Struct. Safety*, **39**, 1-13.

Rossetto, T. and Elnashai, A. (2003), "Derivation of vulnerability functions for European-type RC structures based on observational data", *Eng. Struct.*, **25**(10), 1241-1263.

Saffarini, H.S. (2000), "Ground motion characteristics of the november 1995 aqaba earthquake", *Eng. Struct.*, **22**(4), 343-351.

SAP2000 (2004), *Integrated Software for Structural Analysis & Design*", Computers and Structures Inc., Berkeley, California, U.S.A.

SeismoArtif (2016), *A Computer Program for Generating Artificial Earthquake Accelerograms Matched to a Specific Target Response Spectrum*, SeismoSoft Ltd., Pavia, Italy.

Seleemah, A.A. and El-Sharkawy, M. (2011), "Seismic analysis and modeling of isolated elevated liquid storage tanks", *Earthq. Struct.*, **2**(4), 397-412.

Shakib, H., Omidinasab, F. and Ahmadi, M.T. (2010), "Seismic demand evaluation of elevated reinforced concrete water tanks", *Int. J. Civil Eng.*, **8**(3), 204-220.

Shepherd, R. (1972), "The two mass representation of a water tower structure", *J. Sound Vibr.*, **23**(3), 391-396.

Shome, N. (1999), "Probabilistic seismic demand analysis of nonlinear structures", Ph.D. Dissertation, Stanford University, California, U.S.A.

Sonobe, Y. and Nishikawa, T. (1969), "Study of the earthquake proof design of elevated water tanks", *Proceedings of the 4th World Conference Earthquake Engineering*, Santiago, Chile.

Spritzer, J.M. and Guzey, S. (2017), "Nonlinear numerical evaluation of large open-top aboveground steel welded liquid storage tanks excited by seismic loads", *Thin-Wall. Struct.*, **119**, 662-676.

Steinbrugge, K.V. and Flores, R. (1963), "The Chilean

earthquakes of May, 1960: A structural engineering viewpoint", *Bullet. Seismol. Soc. Am.*, **53**(2), 225-307.
Terenzi, G. and Rossi, E. (2018), "Seismic analysis and retrofit of the oldest R/C elevated water tank in Florence", *Bullet. Earthq. Eng.*, **16**(7), 3081-3102.
Vamvatsikos, D. and Cornell, C.A. (2002), "Incremental dynamic analysis", *Earthq. Eng. Struct. Dyn.*, **31**(3), 491-514.
Veletsos, A.S. and Tang, Y. (1990), "Soil-structure effects for laterally excited liquid storage tanks", *Earthq. Eng. Struct. Dyn.*, **19**, 473-496.

CC